

NEMO/NLK Phosphorylates PERIOD to Initiate a Time-Delay Phosphorylation Circuit that Sets Circadian Clock Speed

Joanna C. Chiu,^{1,2} Hyuk Wan Ko,^{1,3} and Isaac Edery^{1,*}

¹Department of Molecular Biology and Biochemistry, Rutgers University, Center for Advanced Biotechnology and Medicine, Piscataway, NJ 08854, USA

²Department of Entomology, University of California, Davis, Davis, CA 95616, USA

³Present Address: Neurodegeneration Control Research Center, School of Medicine, Kyung Hee University, Seoul 130-701, South Korea

*Correspondence: edery@cabm.rutgers.edu

DOI 10.1016/j.cell.2011.04.002

SUMMARY

The speed of circadian clocks in animals is tightly linked to complex phosphorylation programs that drive daily cycles in the levels of PERIOD (PER) proteins. Using *Drosophila*, we identify a time-delay circuit based on hierarchical phosphorylation that controls the daily downswing in PER abundance. Phosphorylation by the NEMO/NLK kinase at the “per-short” domain on PER stimulates phosphorylation by DOUBLETIME (DBT/CK1 δ/ϵ) at several nearby sites. This multisite phosphorylation operates in a spatially oriented and graded manner to delay progressive phosphorylation by DBT at other more distal sites on PER, including those required for recognition by the F box protein SLIMB/ β -TrCP and proteasomal degradation. Highly phosphorylated PER has a more open structure, suggesting that progressive increases in global phosphorylation contribute to the timing mechanism by slowly increasing PER susceptibility to degradation. Our findings identify NEMO as a clock kinase and demonstrate that long-range interactions between functionally distinct phospho-clusters collaborate to set clock speed.

INTRODUCTION

Circadian ($\cong 24$ hr) rhythms are a widespread feature of the temporal organization exhibited by life forms and are driven by cellular pacemakers or clocks that are based on species- or tissue-specific sets of “clock” genes (Schibler, 2006). A hallmark feature of these clocks is that, even in the absence of external time cues, they oscillate with free-running periods of ~ 24 hr. Based on many lines of evidence obtained from a range of model systems, it is clear that dynamic change in the phosphorylation state of one or more clock proteins is a key “state variable” in rhythm-generating mechanisms driving the pace of these clocks

(Bae and Edery, 2006; Gallego and Virshup, 2007; Markson and O’Shea, 2009; Mehra et al., 2009). In animals, PERIOD (PER) proteins are the clock components behaving as the primary “phospho-timer” (Bae and Edery, 2006; Gallego and Virshup, 2007), whereas in *Neurospora*, it is FREQUENCY (FRQ) (Brunner and Schafmeier, 2006; Heintzen and Liu, 2007; Mehra et al., 2009). Another shared feature of these phospho-timing clock proteins is that they connect to gene expression by functioning in a phase-specific manner to inhibit the activities of positively acting core clock transcription factors, leading to daily cycles in gene expression that ultimately underlie many of the observed circadian rhythms in cellular, physiological, and behavioral phenomena.

How phosphorylation regulates clock speed in eukaryotes is not clear. Recent findings indicate that there are 25–30 phosphorylation sites on PER proteins in animals (Chiu et al., 2008; Vanselow et al., 2006) and 80–100 on FRQ (Baker et al., 2009; Tang et al., 2009), many of which undergo daily changes in phospho-occupancy. The dynamic regulation of PER and FRQ phosphorylation involves multiple kinases and phosphatases (Bae and Edery, 2006; Gallego and Virshup, 2007; Mehra et al., 2009). In these eukaryotic systems, a major effect of phosphorylation on regulating clock pace is via controlling the stabilities of PER and FRQ proteins, which yields daily cycles in their levels that drive clock progression. Studies in *Drosophila melanogaster* have been instrumental in our understanding of clock mechanisms in general and mammalian ones in particular (Allada and Chung, 2010). Indeed, that time-dependent changes in the phosphorylated state of a key clock protein might be a critical aspect of circadian timing mechanisms was initially suggested based on the *Drosophila* PER (dPER) protein, the first clock protein to be biochemically characterized (Edery et al., 1994).

DOUBLETIME (DBT) (homolog of mammalian CK1 δ/ϵ) is the major kinase controlling the temporal program underlying dPER phosphorylation and stability (Kloss et al., 1998; Price et al., 1998). Newly synthesized dPER is initially present as a hypophosphorylated variant(s) in the late day/early night, progressively increasing in extent of phosphorylation such that, by the late night/early day, only hyperphosphorylated species are detected (Edery et al., 1994). During this temporal

phosphorylation program, dPER enters the nucleus around midnight, where it acts to repress the central clock transcription factors dCLOCK (dCLK) and CYCLE (CYC). The F box protein SLIMB (*Drosophila* homolog of β -TrCP) (Grima et al., 2002; Ko et al., 2002) preferentially recognizes highly phosphorylated isoforms of dPER, targeting them for proteasomal degradation, which relieves repression of dCLK-CYC, enabling the next round of circadian transcription. A strikingly similar scenario also occurs in mammals, whereby CK1 δ/ϵ plays a major role in regulating daily cycles in the abundance of mammalian PERs (mPER1–3) by targeting them to the proteasome via β -TrCP (Gallego and Virshup, 2007). The importance of PER phosphorylation to human health is highlighted by studies showing that mutations in either a phosphorylation site on human PER2 or CK1 δ underlie several familial advanced sleep phase syndromes (FASPS) (Toh et al., 2001; Vanselow et al., 2006; Xu et al., 2005, 2007).

Because the daily downswing in the levels of PER proteins coincides with when they attain highly phosphorylated states, it was thought that the targeting of these proteins to the proteasome is based on the recognition of many phosphorylation signals. However, several years ago, we showed that, although the first 100 aa of dPER contain only a fraction of the total phosphorylated residues, the phospho-signals in this region are necessary and sufficient for SLIMB binding (Chiu et al., 2008). Most notably, the phospho-occupancy of Ser47 is the key signal regulating the efficiency of SLIMB binding, a critical event in setting the pace of the clock (Chiu et al., 2008). However, if recognition of clock proteins such as PER to their respective F box proteins only requires a few phosphorylated residues, how do other phosphorylation events contribute to setting the clock speed?

As an entrée into this problem, we sought to understand the role of the classic *per*^{short} (*per*^S) allele, which exhibits behavioral rhythms of ~19 hr (Konopka and Benzer, 1971) and accelerates the biochemical cycles in dPER phosphorylation and abundance (Edery et al., 1994; Marrus et al., 1996). The *per*^S mutation changes a Ser residue at amino acid (aa) position 589 to Asn (S589N) (Baylies et al., 1987; Yu et al., 1987), and recent findings from the Young lab and our group raised the possibility that Ser589 is phosphorylated in vivo (Chiu et al., 2008; Kivimäe et al., 2008). Herein, we show that not only is Ser589 phosphorylated in flies, but that it also functions as part of a hierarchical phospho-cluster. This phospho-cluster is gated by phosphorylation at Ser596, which stimulates the phosphorylation by DBT at the *per*^S site and several nearby Ser/Thr residues. The per-short phospho-cluster functions as a major control center of the dPER phosphorylation program by delaying the timing of DBT-dependent phosphorylation at other more distal regions on dPER, including Ser47. We also show that Ser596 is phosphorylated by the proline-directed kinase, NEMO/NLK, identifying a new kinase in the central clockworks. We propose that time-delay phospho-circuits that slow down phosphorylation at other phospho-clusters are likely to be key aspects of the “timer” in eukaryotic circadian clocks, and we also provide a working model for understanding how mutations in clock protein phosphorylation sites and/or the kinases that phosphorylate them can yield both fast and slow clocks.

RESULTS

The Per-Short Phospho-Cluster Is a Major Determinant Regulating dPER Stability by Controlling the Rate of DBT-Mediated Binding of dPER to SLIMB

Our prior mass spectrometry data indicated that the *per*^S site (Ser589) and several nearby sites (i.e., Ser596, Ser585, and Thr583) are phosphorylated (Chiu et al., 2008), suggesting that this region functions as a discrete phospho-cluster. Indeed, earlier work showed that a variety of missense mutations in the region encompassing aa585–601 of dPER (Figure 1A) lead to short period phenotypes (termed the “per-short domain”) (Baylies et al., 1992; Rothenfluh et al., 2000). As an initial attempt to probe the effects of phosphorylation in the per-short domain, we used a previously described assay based on cultured *Drosophila* Schneider (S2) cells (Ko and Edery, 2005; Ko et al., 2002). In this system, the DBT-dependent progressive phosphorylation and subsequent SLIMB-mediated degradation of dPER can be recapitulated by transfecting S2 cells with recombinant *dper* and *dbt*, whereby expression of *dbt* is controlled by the copper-inducible metallothionein promoter (pMT) and that of *dper* by the constitutive actin5C promoter (pAc).

Replacing each of the phosphorylated Ser/Thr residues in the per-short domain that we identified by mass spectrometry to an Ala [dPER(TS583-596A)] greatly accelerated the timing of DBT-mediated degradation of dPER (Figures 1B and 1D and Figure S1A). In addition, the transition from hypo- to hyperphosphorylated dPER isoforms occurs earlier, with slowly migrating species of dPER(TS583-596A) readily visible 6 hr after *dbt* induction (Figure 1B, compare lanes 2 and 6). The kinetics of DBT-mediated phosphorylation and degradation were still accelerated when the Ser/Thr phospho-acceptor sites in the per-short domain were replaced with Asp [dPER(TS583-596D)], suggesting that, in this case, the negatively charged Asp residues do not function as phospho-mimetics (Figure 1B, lanes 13–16). Our results are consistent with recent findings showing that deletion of the per-short domain renders dPER less stable when expressed in S2 cells (Kivimäe et al., 2008).

We next replaced individual phospho-acceptor sites in the per-short domain with an Ala residue. In addition, we evaluated another per-short domain mutant called *per*^T (G593D), which yields a severe short phenotype with 16 hr behavioral rhythms (Hamblen et al., 1998; Konopka et al., 1994) (Figure 1A). All of the different versions of dPER were degraded faster except for dPER(T583A), which behaved similar to that of wild-type dPER (Figures 1C and 1D and Figure S1B available online). Intriguingly, there is a clear trend toward faster DBT-mediated degradation for mutations closer to the carboxy (C)-terminal end of the per-short domain, with dPER(S596A) showing the greatest instability among the single-site mutants (Figure 1D; e.g., compare values at 6 hr post-*dbt* induction). A C-terminal bias in the rate of DBT-induced increases in dPER phosphorylation was also observed in the presence of MG132 to inhibit proteasome-mediated degradation (Figure 2A and Figures S2A and S2B; see Figure S2B for measurement of a hyperphosphorylation index). Because all of the different dPER versions are eventually converted to hyperphosphorylated isoforms when degradation is inhibited (Figure 2A and Figure S2A), these results indicate that

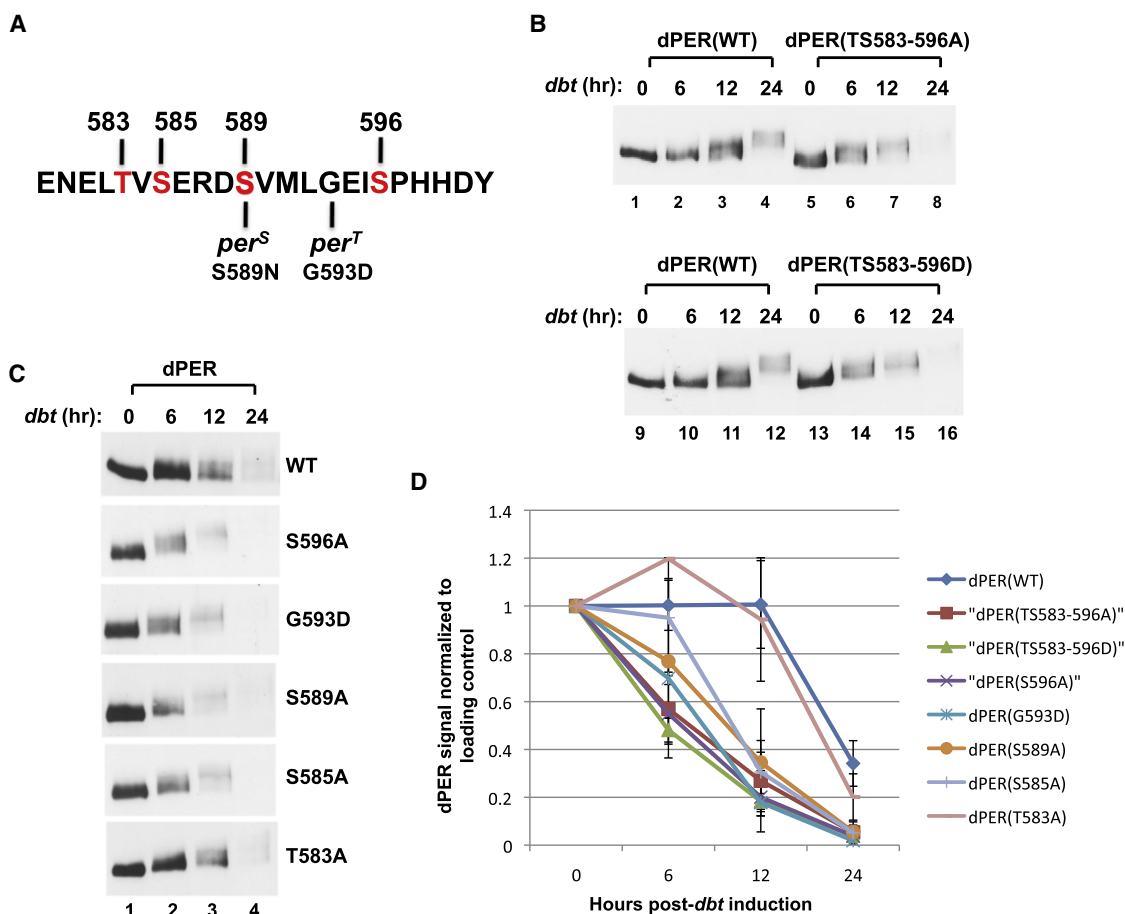


Figure 1. Differential Effects of Phospho-Site Mutations in the *per^S* Phospho-Cluster on DBT-Dependent Phosphorylation Kinetics and Degradation Rate of dPER in Cultured S2 Cells

(A) Sequence of dPER from amino acid 579 to 601, encompassing the original “*per*-short” region (aa 585 to 601), highlighting the phosphorylation site mutations generated in this study (labeled in red) as well as locations of the *per^S* and *per^T* mutations.

(B and C) S2 cells were cotransfected with wild-type (WT) or mutant variants of pAc-3XFLAG-His-*dper*-6Xcmv (simplified as *dper*) and pMT-*dbt*(WT)-V5-His (simplified as *dbt*, left of panels) and collected at the indicated times (hr) post-*dbt* induction. The dPER variants (top of panels) were detected by immunoblotting in the presence of α -*c-myc* antibodies.

(D) dPER staining intensity values normalized to Hsp70 loading control. At least two independent experiments were used to generate the average for each time point.

Error bars represent SEM. See Figure S1 for supporting data.

the *per*-short domain functions in a spatially oriented manner to regulate the rate by which DBT progressively increases the global phosphorylation of dPER, whereby eliminating phosphorylation at sites closer to the C terminus of this cluster leads to faster kinetics.

Although DBT phosphorylates dPER at numerous regions, phosphorylation events in the first 100 aa of dPER are sufficient and necessary for SLIMB binding, with phosphorylation at Ser47 being a critical signal generating the SLIMB phospho-degron (Chiu et al., 2008). Identification of the SLIMB-binding site on dPER was partly accomplished by generating a “TEV/TAG” version of dPER, which contains a FLAG epitope at the amino terminus and a TEV protease site inserted at aa 100 (dPER/TEV100) (Chiu et al., 2008). This strategy enables the normal phosphorylation of full-length dPER in S2 cells followed by extract preparation and TEV cleavage to determine the biochem-

ical properties of the aa 1–100 SLIMB-binding fragment in isolation. We applied this approach to probe whether the *per*-short phospho-cluster affects phosphorylation within the first 100 aa by generating TEV/TAG versions of different *per*-short domain mutants under conditions whereby S2 cells were incubated with MG132 to block degradation. A trend toward more C-terminal phospho-site mutants exhibiting faster DBT-mediated phosphorylation kinetics was also observed for the first 100 aa of dPER (Figure 2B, top, and Figure S2C). For example, at 6 hr post-*dbt* induction, there is clearly a higher fraction of hypophosphorylated to hyperphosphorylated isoforms in the first 100 aa of wild-type dPER compared to the S596A and S589A versions (Figure 2B, top, compare lanes 2, 6, 10, and 14, and Figure S2C). To further link phosphorylation at the *per*-short domain to SLIMB-mediated events, we evaluated a double mutant whereby phosphorylation at S47 and S596 is abolished

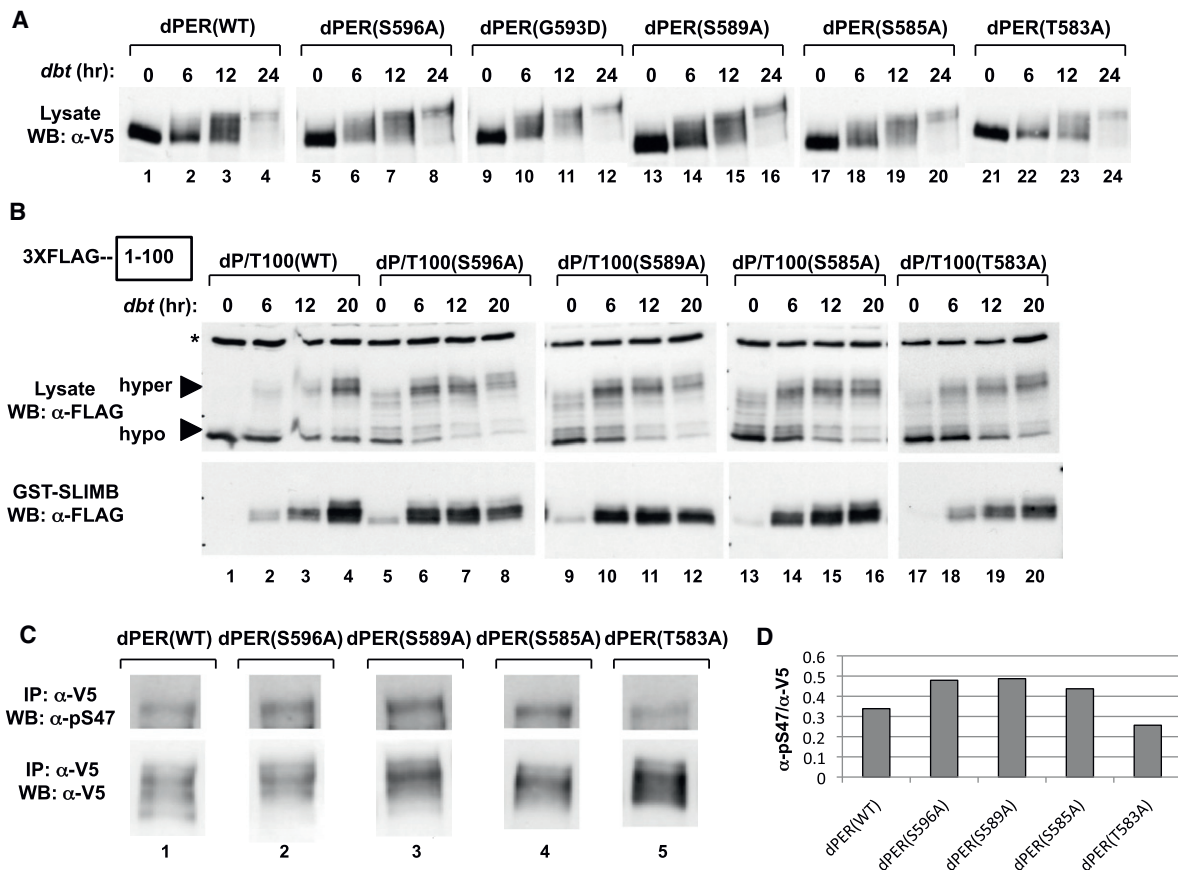


Figure 2. Differential Effects of Phospho-Site Mutants in the *per*^S Phospho-Cluster on dPER/SLIMB Interactions and S47 Phosphorylation
 (A) S2 cells were cotransfected with *dbt* and *dper* (pAc-dper-V5-His) variants and collected at the indicated times (hr) post-*dbt* induction (top of panels). The culture media contained MG132 to inhibit degradation of dPER. The dPER variants were visualized by western blotting (WB) using anti-V5 antibodies.
 (B) S2 cells were cotransfected with WT or mutant variants of pAc-3XFLAG-His-*dper*/Tev100-6Xc-myc and pMT-*dbt*-V5-His, treated with MG132, and collected at the indicated times (hr) post-*dbt* induction (top of panels). Extracts were subjected to TEV protease cleavage. Equal amounts of cleaved protein were incubated with glutathione resins bound with GST-SLIMB. The relative amounts of the dPER(aa 1–100) fragment in the starting material (lysate, top) and that bound to the resins (GST-SLIMB, bottom) were visualized by immunoblotting in the presence of α -FLAG antibodies. Nonspecific bands in the lysate (top) are marked by an asterisk (*, left of panel).
 (C) S2 cells coexpressing pAc-*dper*-V5-His (WT and mutants) and pMT-*dbt*-V5-His were incubated with MG132 and harvested at 6 hr post-*dbt* induction. Extracts were immunoprecipitated (IP) with α -V5 antibodies and dPER isoforms phosphorylated at Ser47 detected using α -pS47 antibodies (top), whereas total dPER protein was visualized using α -V5 antibodies (bottom).
 (D) dPER total protein and pS47 signal intensity in (C) were quantified, and the ratio of dPER pS47 over total dPER proteins was presented in histogram format. See Figure S2 for supporting data.

[dPER(S47/596A)] (Figure S3). Prior work showed that highly phosphorylated species of dPER are stabilized and accumulate if phosphorylation at S47 is blocked [dPER(S47A)] (Chiu et al., 2008). This was also the case for dPER(S47/596A) (Figure S3, compare lanes 4, 8, 12, and 16), indicating that the enhanced degradation of dPER by blocking phosphorylation at S596 is linked to the phosphorylated status at S47.

To evaluate the effects of the *per*-short phospho-cluster within a more functional context, we measured binding of the dPER(aa 1–100) fragment to SLIMB fused to glutathione S-transferase (GST) (Chiu et al., 2008). For the wild-type dPER(aa 1–100) fragment, peak binding to SLIMB occurs at 20 hr post-*dbt* induction, a pattern also observed for the T583A mutant (Figure 2B, bottom, compare lanes 1–4 with 17–20; see Figure S2D for quantitation of

results). In sharp contrast, binding of the 1–100 aa fragment from the S596A and S589A dPER mutants to SLIMB peaks much earlier by 6–12 hr post-*dbt*, whereas maximal binding is attained by 12 hr post-*dbt* induction for the S585A mutant (Figure S2D). Strikingly, although little binding occurred in the absence of exogenous *dbt* (naive S2 cells have some levels of endogenous *dbt*), relative differences were still observed in the binding affinities of the different 1–100 aa dPER fragments to SLIMB, with the S585A mutation yielding less binding compared to the S596A and S589A versions but more than wild-type and the T583A mutation (Figure 2B, bottom, compare lanes 1, 5, 9, 13, and 17). Finally, we also compared the intensity of Ser47 phosphorylation at 6 hr post-*dbt* induction using our previously generated phospho-specific antibodies (Chiu et al., 2008). Even though it

was difficult to obtain a clear order between the mutants (e.g., dPER[S596A] isoforms phosphorylated at Ser47 are relatively more unstable compared to the other dPER variants evaluated even in the presence of proteasome inhibitors; data not shown), the results consistently indicated higher phospho-occupancy of Ser47 for the S596A, S589A, and S585A mutants compared to the wild-type control or dPER(T583A) (Figures 2C, top, and 2D).

In summary, although there is some variation in the relative ordering of mutants depending on the experimental platform used, the cumulative biochemical data indicate that the per-short phospho-cluster is a major determinant of dPER stability by functioning in a spatially oriented and graded manner to regulate the rate of DBT-mediated phosphorylation events underlying the binding of SLIMB to dPER, with phospho-sites closer to the C-terminal side of the cluster having more potent effects.

The Per-Short Domain Is a Time-Delay Phospho-Cluster that Slows Down the Pace of the Clock in a Spatially Oriented and Graded Manner

To investigate the physiological significance of our findings in whole animal systems, we generated transgenic flies that produce tagged versions of the dPER(TS583-596A), dPER(S596A), dPER(S589A), and dPER(S585A) proteins. We did not generate a dPER(T583A) version because the biochemical results indicated no observable differences with control dPER (Figure 1 and Figure 2). The effects of the different transgenes were examined in the *per* null *wper^D* (Konopka and Benzer, 1971), whereby the only functional copy of *dper* is provided by the transgene.

As previously shown, *wper^D* flies expressing the wild-type *dper* transgene exhibit strong rhythms with ~24 hr periods (Figure 3 and Table S1) (Kim et al., 2007; Ko et al., 2007). Also as expected, the p{*dper*(S589A)} transgenic flies, which replace the Ser at the *per^S* site with Ala, manifest ~19 hr rhythms that are similar in length to the original *per^S* mutant (Konopka and Benzer, 1971; Rutila et al., 1992). Flies bearing *dper* transgenes that either abolish phosphorylation at all of the Ser/Thr residues within the per-short phospho-cluster identified by mass spectrometry [p{*dper*(TS583-596A)}] or just Ser596 [p{*dper*(S596A)}] manifested ultrashort behavioral rhythms of ~16 hr. Intriguingly, p{*dper*(S585A)} flies had less severe period-shortening effects with rhythms of ~21 hr. We also evaluated the p{*dper*(TS583-596A)} transgene in a wild-type *per⁺* background and obtained a period of ~21 hr (Table S1), consistent with the semi-dominant nature of *dper* alleles (Konopka and Benzer, 1971). The ability of the different *dper* versions to shorten behavioral rhythms is ordered as follows: p{*dper*(TS583-596A)} = p{*dper*(S596A)} > p{*dper*(S589A)} > p{*dper*(S585A)} > p{*dper*(WT)}.

These findings reveal a remarkable congruence between the period-altering effects of mutations in the per-short phospho-cluster on behavioral rhythms and the biochemical results obtained when analyzing the same dPER versions in cultured S2 cells. Thus, the effects of the per-short phospho-cluster on the speed of circadian pacemakers in flies are closely linked to attenuating the efficiency of DBT-dependent binding of SLIMB to dPER. In addition, blocking phosphorylation at Ser596 eliminates the function of the entire cluster, suggesting that the

16 hr rhythms observed in the *per^T* mutant (G593D) are due to a similar biochemical defect.

Under standard entraining conditions of 12 hr light:12 hr dark cycles (LD) at 25°C, *D. melanogaster* manifest a bimodal distribution of locomotor activity, with a “morning” peak centered around the dark-to-light transition and an “evening” peak centered around the light-to-dark transition (Rosato and Kyriacou, 2006) (Figures 3A–3E, right). As expected, the shorter the free-running period of the dPER mutant, the earlier the timing of evening activity in LD cycles. Daily cycles in dPER abundance and phosphorylation were also advanced in LD, consistent with the behavioral results and prior findings analyzing the *per^S* and *per^T* mutants (Figures 3A–3E, left, and Figures 4C–4E, top; see Figure 3F for quantitation of dPER abundance rhythms) (Edey et al., 1994; Hamblen et al., 1998; Marrus et al., 1996). In this analysis, we collected flies every 4 hr during a daily cycle, precluding a more reliable comparison of the different per-short phospho-cluster mutants.

Phosphorylation at Ser596 Enhances Subsequent Phosphorylation of Ser589 by DBT

To confirm and better analyze individual phosphorylation events within the per-short phospho-cluster, we sought to generate phospho-specific polyclonal antibodies and were successful in generating good quality antibodies that recognize phosphorylated S589 and S596 (α -pS589 and α -pS596). Several lines of evidence demonstrate the high specificity of our α -pS589 and α -pS596 antibodies for phosphorylated Ser589 and Ser596, respectively (Figure 4, Figure S4, and data not shown). For example, phosphatase treatment of wild-type dPER expressed in either S2 cells or flies either eliminated or strongly diminished detection by these antibodies (Figures 4A, compare lanes 3 and 4 to 1 and 2, top two panels, and 4B, compare lanes 3 and 4 to 1 and 2, top two panels). In addition, the staining intensities of dPER(S589A) and dPER(S596A) mutant proteins produced in flies and S2 cells were severely diminished when probed with their respective phospho-specific antibodies (Figures 4C–4E and Figure S4).

Results obtained using mass spectrometry of dPER produced in either S2 cells or phosphorylated in vitro in the presence of DBT strongly suggest that the *per^S* site is phosphorylated by DBT (Chiu et al., 2008; Kivimäe et al., 2008), consistent with earlier work demonstrating allele-specific genetic interactions between a presumed hypomorphic allele of *dbt*, termed *dbt^{AR}*, and the *per^S* mutation (Rothenfluh et al., 2000). Indeed, induction of *dbt* in S2 cells greatly enhanced phosphorylation of Ser589 (Figure 4A, top, compare lanes 1 and 2). We also generated an α -pS585 antibody that unfortunately only resulted in a detectable signal when probing dPER produced in S2 cells. Nonetheless, like pS589, the intensity of the signal was strongly increased following induction of *dbt* (Figure S5A, compare lanes 1 and 2, top). In contrast, the Ser residue at position 596 is followed by a “pro-directed” kinase, making it highly unlikely that DBT directly phosphorylates S596 (discussed below). Furthermore, mass spectrometry analysis shows that, unlike S589, S585, and T583, induction of exogenous *dbt* is not required to detect phosphorylated S596 (Chiu et al., 2008), indicating the presence

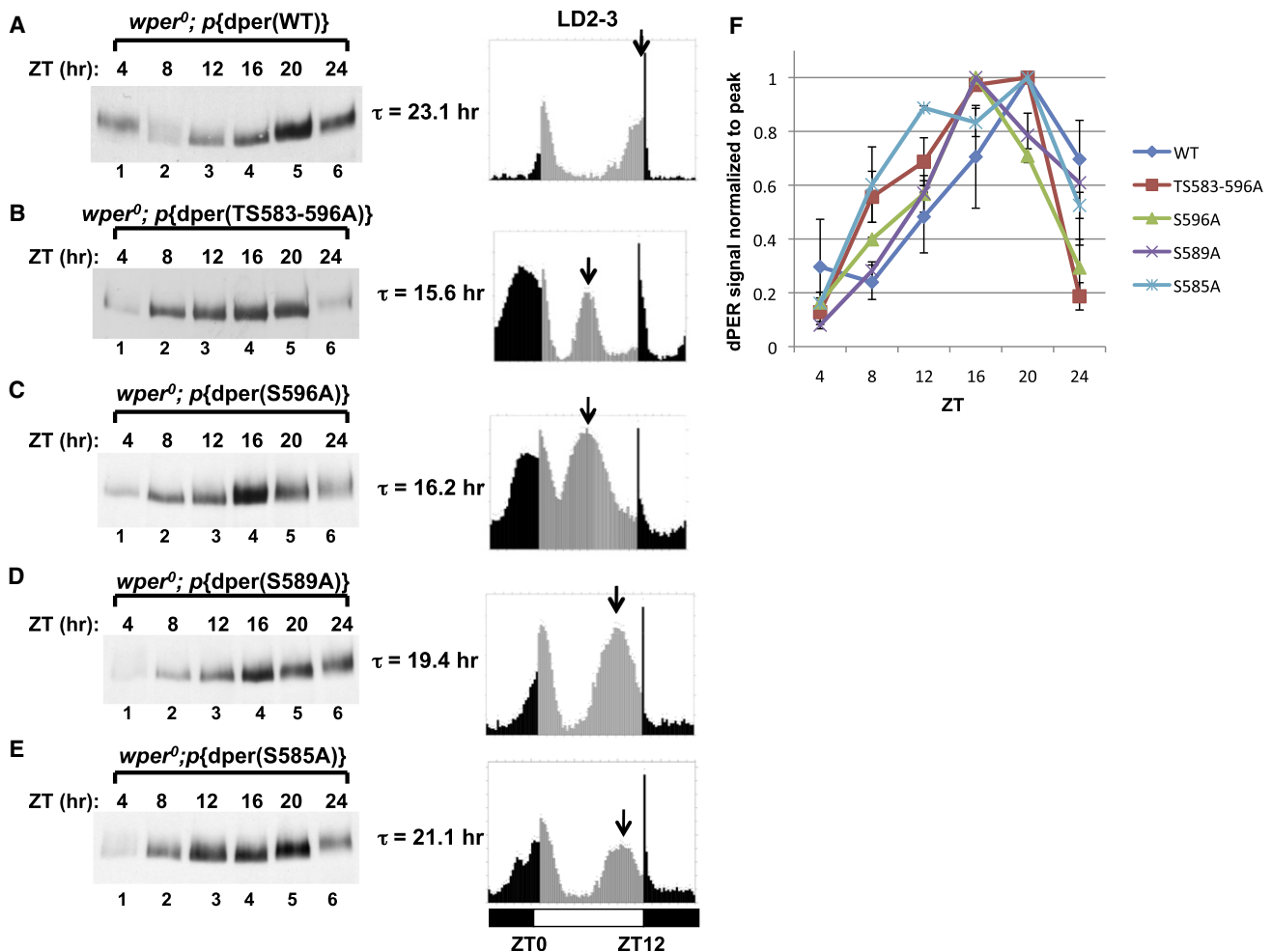


Figure 3. Spatially Oriented and Graded Responses of Per-Short Phospho-Cluster Site Mutants on Clock Speed

(A–E) (Left) Flies bearing different *dper* transgenes (indicated at top of panels) in a *wper⁰* genetic background were collected at the indicated times (top of panels), and head extracts were analyzed for dPER by immunoblotting in the presence of α -HA. (Right) The corresponding locomotor activity profiles of the transgenic flies in LD are shown. The second and third days worth of activity data during LD were averaged, generating the 24 hr profiles shown in the panels. The free-running periods (τ) are also shown. Arrow represents the timing of the clock-controlled evening peak. Vertical bars represent the activity recorded in 15 min bins during times when the lights were on (gray bars) or off (black bars). ZT0 is lights on, whereas ZT12 is lights off. Horizontal bars at bottom; open, lights-on; closed, lights-off.

(F) dPER signal intensity (y axis) was normalized by setting the peak intensity value for each dPER variant to a value of 1. Two independent experiments were used to generate the average, and error bars represent SEM.

See Table S1 for supporting data.

of one or more endogenous kinase(s) in S2 cells that can modify S596 (see below). In agreement with this notion, phosphorylated Ser596 is readily detected when S2 cells are singly transfected with only *dper*-containing plasmids (Figure 4A, middle, compare lanes 1 and 2).

To investigate whether Ser589 is phosphorylated in a DBT-dependent manner in vivo, we used transgenic flies bearing the dPER(Δ dPDBD) internal deletion (Figure 4B), which removes aa 755–809 of dPER and abrogates the ability of DBT to stably bind and phosphorylate dPER (Kim et al., 2007; Nawathean et al., 2007). Indeed, whereas the intensity of phosphorylated Ser589 in the delta mutant is reduced to phosphatase treated nonspecific background levels (Figure 4B, top, compare lanes

5 and 6 to 7 and 8), phosphorylation at Ser596 remains strong (Figure 4B, middle, compare lanes 5 and 6 to 7 and 8).

Remarkably, blocking phosphorylation at S596 abolished phosphorylation at S589 in flies (Figure 4D) and strongly delayed the kinetics of DBT-mediated phosphorylation at S589 in S2 cells (Figure S4). In sharp contrast, the phosphorylated status of S589 has no bearing on the efficiency of phosphorylation at S596 (Figure 4E; see also Figure 6B and Figure S4). A similar relationship was also observed for S585, whereby phosphorylation of S596 in flies was normal in the dPER(S585A) mutant (Figure S5B, middle), and in cultured S2 cells, S596 strongly enhances phosphorylation at S585 (Figure S5A, top, compare lanes 2 and 14). Although blocking phosphorylation at S589 does not impede

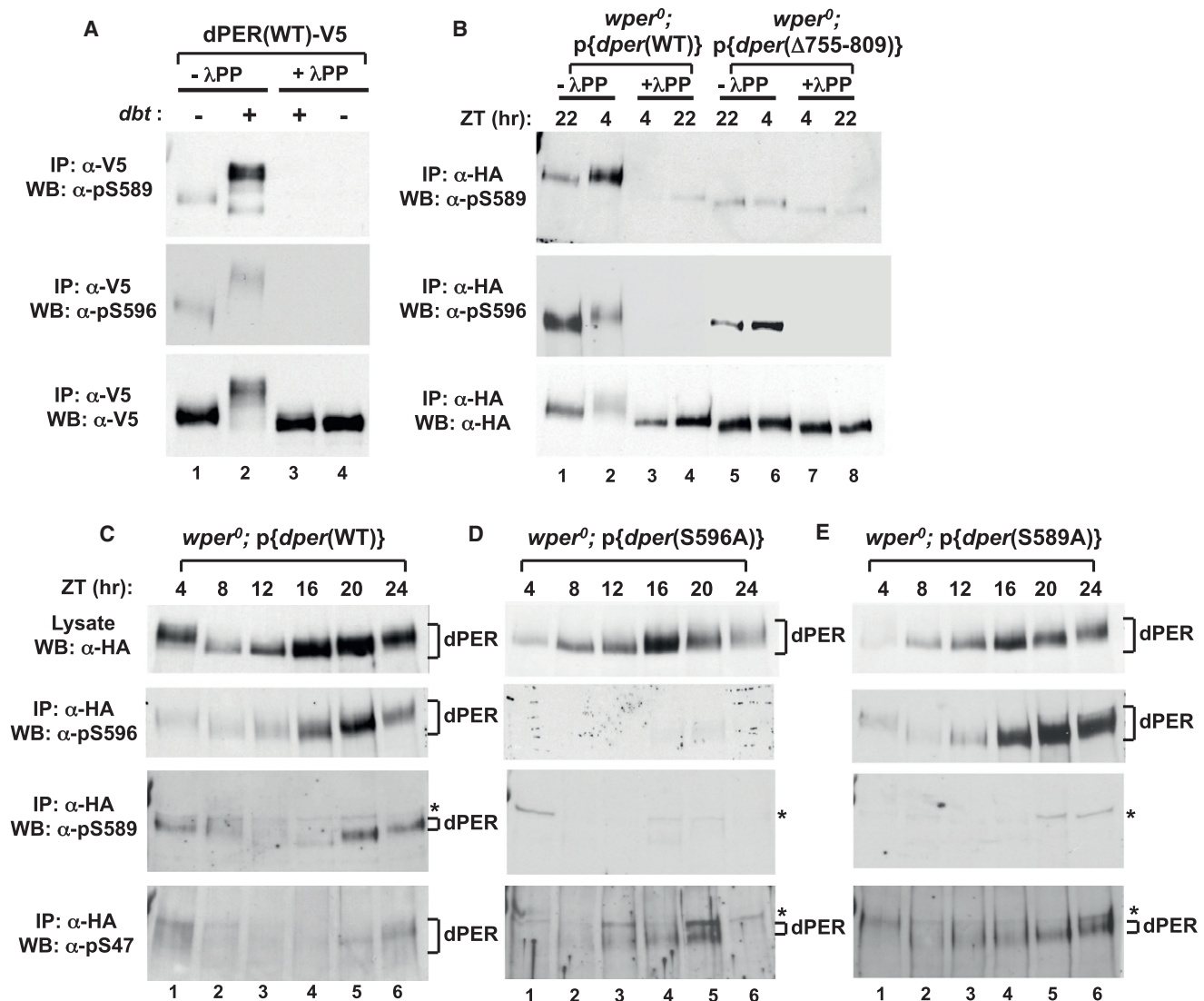


Figure 4. Phospho-Specific Antibodies Reveal that DBT Phosphorylates S589, but Not S596, and that Phosphorylation at S596 Stimulates Phosphorylation at S589 and S585, Which Delays Phosphorylation at S47

(A) Extracts were prepared from S2 cells cotransfected with a wild-type (WT) version of *dper* (*pAc-dper-V5-His*) and *pMT-dbt-V5-His* (+) or an empty *pMT* plasmid, *pMT-V5-His* (–). Cells were treated with MG132 and cycloheximide 16 hr post-*dbt* induction and harvested 4 hr later. dPER was immunoprecipitated (IP) with α -V5 beads and split into equal parts that were either treated in the absence (– λ PP) or presence (+ λ PP) of λ -phosphatase. Recovered immune complexes were probed by western blotting (WB) in the presence of the indicated antibody (left of panel).

(B) Head extracts were prepared from *wper*⁰;*p{dper(WT)}* or *wper*⁰;*p{dper(Δ 755-809)}* flies collected at the indicated times (ZT; top of panels). dPER-HAHis-containing immune complexes were recovered using α -HA beads and split into two equal parts that were treated in the absence (– λ PP) or presence (+ λ PP) of λ -phosphatase. Recovered immune complexes were probed by western blotting (WB) in the presence of the indicated antibody (left of panel).

(C–E) Head extracts were prepared from *wper*⁰;*p{dper(WT)}*, *wper*⁰;*p{dper(S589A)}*, and *wper*⁰;*p{dper(S596A)}* flies collected at the indicated times (ZT). dPER-HAHis-containing immune complexes were recovered using α -HA beads, followed by western blotting (WB) in the presence of the indicated antibody (left of panel). Positions of nonspecific signals from α -pS589 and α -pS47 antibodies are indicated by asterisks (*; right of panels).

See Figure S4 and Figure S5 for supporting data.

phosphorylation at S585, and vice-versa, it is possible that blocking one site reduces phosphorylation at the other site (Figures S5A, compare lanes 2 and 10, top, and S5B, bottom). Immunoblotting of extracts prepared from wild-type flies collected at different times in a daily cycle shows that phosphorylation at S596 precedes that at S589 and that phosphorylation at S589 peaks prior to that of S47 (Figure 4C). Moreover, dPER

isoforms containing phosphorylated S47 are readily observed by ZT12–16 for the S596A and S589A dPER mutants, whereas detection of pS47 for wild-type dPER begins around ZT20 and peaks in the early day (Figures 4C–E). This striking temporal order is further evidence for a model whereby phosphorylation of S596 enhances phosphorylation by DBT of S589 and presumably the other phospho-acceptor sites on the per-short cluster

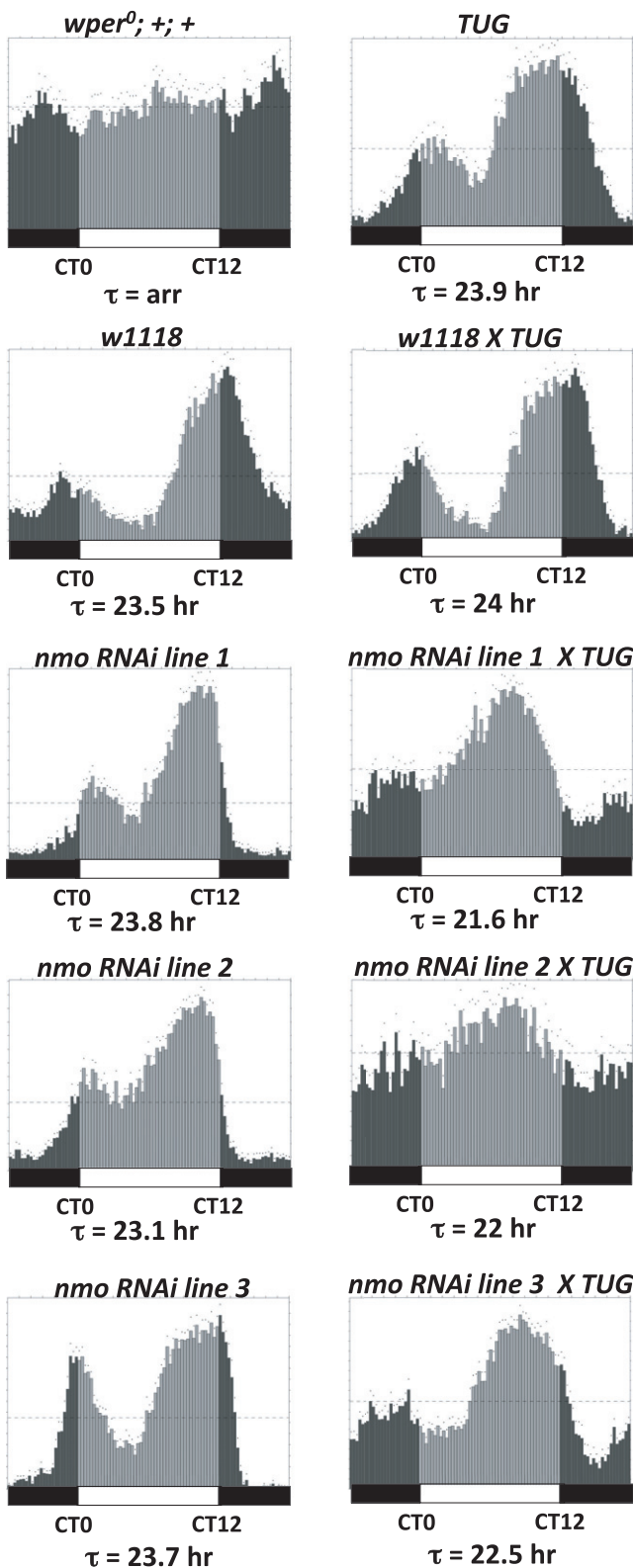


Figure 5. RNAi Knockdown of *nmo* in Pacemaker Cells Speeds Up the Pace of the Clock

Shown are group averages of the 24 hr activity profiles (average of first 3 days during constant dark conditions) for males of the different genotypes. The free-running periods (τ) are also shown. Vertical bars represent the activity recorded in 15 min bins during the subjective day (light gray bars; CT0-12) or subjective night (dark gray bars; CT12-24). Horizontal bars at bottom; open, subjective day; closed, subjective night. Targeted expression of *nmo* RNAi in *tim*-expressing clock neurons was achieved using the UAS/GAL4 system. The GAL4 driver line used here is *w; UAS-DICER2; tim-UAS-GAL4* (TUG). Three independent responder RNAi lines (line 1 = v101545, line 2 = v104885, line 3 = v3002) were used, and they were all in *w¹¹¹⁸* genetic background. Appropriate parental and genetic background (*w¹¹¹⁸*) controls were included in the experiment. *wper⁰; +; +* represents the control for arrhythmicity (arr).

domain (i.e., S585 and possibly T583), which collectively act to delay DBT-mediated phosphorylation at the SLIMB recognition site on dPER centered on the phospho-occupancy of S47.

NEMO/NLK Kinase Phosphorylates Ser596

As noted above, the Ser residue at position 596 of dPER is followed by a proline residue, indicating that Ser596 is phosphorylated by a pro-directed kinase. These kinases are part of the CMGC family of kinases that include several subfamilies, such as mitogen-activated protein kinases (MAPK), cyclin-dependent kinases (Cdks), and dual-specificity tyrosine-regulated kinases (DYRKs) (Kannan and Neuwald, 2004). Based on sequence motifs, there are ~34 known/predicted CMGC kinases in *Drosophila melanogaster* (<http://www.kinase.com>). It is unlikely that the kinase phosphorylating S596 would be from outside of the CMGC family, as the flanking Pro residue on the substrate greatly constrains the kinds of kinases that can recognize and phosphorylate the amino-proximal Ser/Thr acceptor site (Kannan and Neuwald, 2004).

To try to identify physiologically relevant kinases that might phosphorylate Ser596, we used the Gal4/UAS system (Brand and Perrimon, 1993) to screen available transgenic RNAi lines from the Vienna-based *Drosophila* stock center (VDRC) (Dietzl et al., 2007) that were directed against known/predicted *Drosophila* CMGC kinases. We used the well-characterized *tim-UAS-Gal4* driver (TUG) (Blau and Young, 1999) to drive RNAi expression in clock cells (TUG > UAS-RNAi). We reasoned that inhibiting expression of the Ser596 kinase in clock cells should, at least partially, phenocopy the S596A mutation and yield behavior rhythms with short free-running periods. Of all of the RNAi lines that we tested, only those targeting the kinase NEMO (NMO) manifested significantly short periods compared to parental controls (Figure 5 and data not shown). Three independent TUG > UAS-*nmo*RNAi lines yielded free-running periods of ~21–22 hr (Figure 5). Although the 21–22 hr rhythms observed in *nmo* RNAi flies are not as short as the ~16 hr periods observed in *p{dper(S596A)}* flies, severe *nmo* hypomorphs also manifest 21–22 hr rhythms (Yu et al., 2011). Thus, it is highly unlikely that the 21–22 hr rhythms observed using three independent *nmo* RNAi lines are because of incomplete silencing of *nmo*. Also, NMO might phosphorylate other sites on dPER and/or other clock proteins, which could explain why reducing its levels/activity does not have equivalent effects on clock speed

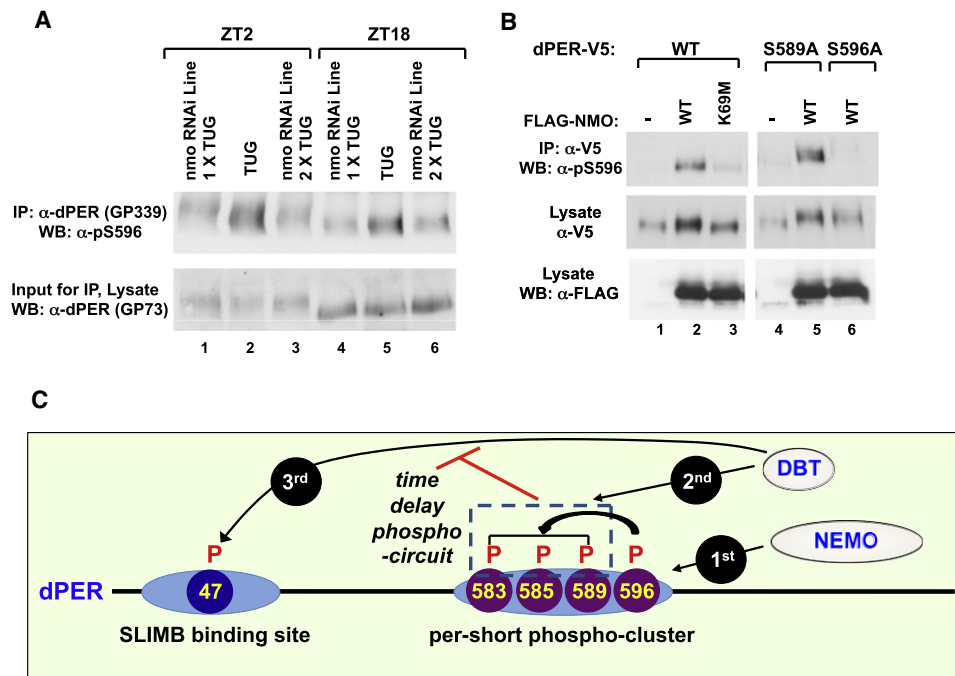


Figure 6. NMO Is a Clock Kinase that Phosphorylates S596 on dPER

(A) Targeted expression of *nmo* RNAi in *tim*-expressing clock neurons was achieved by crossing *w; UAS-DICER2; tim-UAS-GAL4* (TUG) males with females from two independent responder RNAi lines (v101545 [line 1] and v104885 [line 2]) that are in a *w¹¹¹⁸* genetic background. Flies were collected at ZT 2 or 18 and head extracts prepared. dPER-containing immune complexes were recovered using α -dPER antibodies (GP339), followed by western blotting (WB) with α -pS596 (top). The relative input of dPER for the IP was assayed by western blotting (WB) with α -dPER (GP73; bottom).

(B) S2 cells were transfected with pAc-*dper*-V5-His (WT, S589A, or S596A mutant) in the presence of an empty plasmid (pAc-3XFLAG-His) or *nmo*-expressing plasmid (pAc-3XFLAG-His-*nmo* [WT or K69M kinase-dead mutant]). dPER-V5-containing immune complexes were recovered using α -V5 beads, followed by western blotting (WB) in the presence of the indicated antibody (left of panel) to detect dPER isoforms phosphorylated at S596 (top), total dPER proteins (middle) and NMO (bottom).

(C) Model showing how the *per*-short phospho-cluster regulates the pace of the clock. NMO phosphorylates S596 on dPER, which stimulates DBT-dependent phosphorylation of S589, S585, and (perhaps) T583. Phosphorylation in the *per*-short phospho-cluster somehow delays phosphorylation at other DBT-dependent sites on dPER, including S47, thus delaying the dPER/SLIMB interaction and the daily downswing in dPER levels.

See Figure S4, Figure S5, and Figure S6 for supporting data.

as eliminating phosphorylation at S596 (Figure 6B and data not shown). Genetic manipulations using the UAS/GAL4 system to overexpress *nmo* in clock cells did not lead to significant changes in behavioral periods, suggesting that its levels are not rate limiting for clock speed (data not shown).

To verify that NMO phosphorylates S596 in flies, we generated head extracts from TUG > UAS-*nmo*RNAi flies and parental controls collected at ZT18 and ZT2 and probed by immunoblotting in the presence of phospho-specific α -pS596 antibodies. Two different *nmo*RNAi lines were evaluated to ensure reproducibility. Expressing RNAi directed against *nmo* in clock cells led to striking decreases in the staining intensity of phosphorylated S596 (Figure 6A, top, and Figure S6E, middle) that are not due to variations in the total abundance of dPER (Figure 6A and Figure S6E, bottom). We also evaluated the status of phosphorylation at S589, which is readily observed at ZT2, but not ZT18, in control flies (Figure S6E, top). Importantly, the phospho-occupancy of S589 is also diminished in the *nmo* RNAi lines (Figure S6E, compare lanes 1–3), further establishing that, in flies, phosphorylation of S596 by NMO stimulates downstream phosphorylation of S589.

Additional evidence for NMO as a dPER kinase was obtained in cultured S2 cells and in vitro (Figure 6 and Figure S6). For example, expression of wild-type NMO in S2 cells, but not a negative-dominant version (K69M), increased phosphorylation of S596 in wild-type dPER (Figure 6B, lanes 1–3, and Figure S6B), whereas no phospho-specific signal was observed with the S596A mutant (Figure 6B, compare lanes 2 and 6, and Figure S6B, compare lanes 2 and 5). It is noteworthy that NMO still evokes a mobility shift in the dPER(S596A) mutant (Figure 6B, middle, lanes 4–6), suggesting additional phosphorylation sites on dPER (data not shown). Blocking phosphorylation at S589 does not affect phosphorylation at S596 by NMO (Figure 6B, lanes 4 and 5). We also expressed all of the known/suspected pro-directed kinases, and only induction of *nmo* led to significant increases in the phospho-occupancy of S596 (Figure S6A and data not shown). In agreement with this observation, dPER specifically interacts with NMO, but not other kinases of the CMGC family (Figure S6C). To obtain more direct evidence that NMO phosphorylates S596, dPER was purified and phosphatase treated to remove any phosphorylation that occurred in S2 cells and was subsequently incubated with a range of

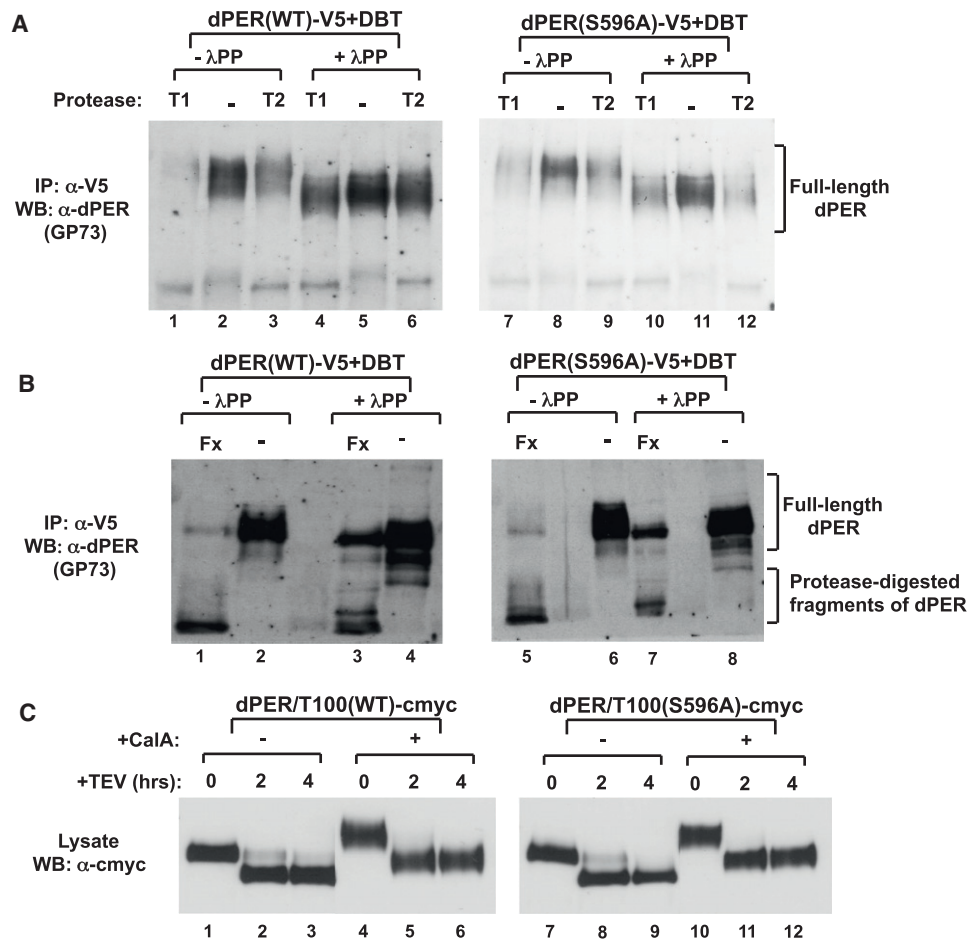


Figure 7. Limited Proteolysis Suggests that Highly Phosphorylated dPER Has a More Open Conformation Compared to Hypophosphorylated Isoforms

(A and B) Extracts were prepared from S2 cells cotransfected with WT or S596A variants of *pAc-dper-V5-His* and *pMT-dbt* that were harvested 20 hr after *dbt* induction. dPER protein was immunoprecipitated (IP) with α-V5 beads and subsequently treated in the absence (–λPP) or presence (+λPP) of λ-phosphatase. Immunoblotting with α-dPER antibodies was used to detect dPER proteins after limited proteolysis using (A) Trypsin (T1 and T2) or (B) Factor Xa (Fx).

(C) Extracts were prepared from S2 cells transfected with WT or S596A variants of *pAc-dper/Tev100-V5-His*. Hyperphosphorylated dPER was generated by addition of 30 nM of Calyculin A (Calbiochem) 2 hr before cell harvest. 50 μM MG132 (Sigma) and 10 μg/ml cycloheximide (Sigma) were also added to maximize the amount of hyperphosphorylated dPER and to prevent degradation. Cells were harvested 48 hr after transfection. Immunoblotting with α-c-myc antibodies was used to detect dPER (full-length and aa 101–1224) proteins after limited proteolysis using AcTEV (Invitrogen).

commercially available kinases, including the highly structurally related MAP kinase. Of all of the kinases that we tested in vitro, only NMO led to dramatic increases in the phospho-occupancy of S596 (Figure S6D).

Phosphorylation-Induced Conformational Changes

While the phospho-occupancy of Ser47 plays a critical role in the direct binding of SLIMB to dPER, a general role of global phosphorylation might be to evoke conformational changes that slowly make dPER a more efficient substrate for degradation. As an initial attempt to address this issue, we purified hyperphosphorylated dPER and treated part of the sample with phosphatase to reduce/eliminate phosphorylation, whereas the other part was mock treated. Finally, both samples were subjected to limited proteolysis using a variety of proteases. Intriguingly, hyperphosphorylated dPER is more susceptible to degradation,

implying a more open structure (Figures 7A and 7B). This was also the case when using the TEV protease with our dPER/T100 version of dPER. For example, some full-length dPER/T100 is still observed after 2 hr incubation with TEV for the hypophosphorylated version, whereas little to no full-length product is detected in the hyperphosphorylated version (Figure 7C, compare lanes 2 and 5), suggesting that the region encompassing the SLIMB-binding region in the first 100 aa is also more accessible in highly phosphorylated dPER. Similar results were also obtained when we compared hyper- and hypophosphorylated isoforms of the dPER(S596A) mutant (Figure 7). Using this assay, we were not able to observe a reproducible difference in the susceptibility to limited proteolysis between wild-type dPER and dPER(S596A). Although this experimental strategy does not provide high-resolution structural information, the results are consistent with the notion that the more rapid DBT-mediated

degradation kinetics for dPER(S596A) (Figure 1) is not due to a grossly different conformation compared to wild-type dPER but, rather, due to changes in the speed with which the mutant version attains isoforms more prone to degradation.

DISCUSSION

Herein, we show that the per-short domain functions as a discrete hierarchical phospho-cluster that delays DBT-mediated phosphorylation at the SLIMB recognition site on dPER, providing new insights into how clock protein phosphorylation contributes to circadian timing mechanisms (Figure 6C). The cumulative effect of this delay circuit is to slow down the pace of the clock by ~8 hr. We propose that DBT functions in a stepwise manner to phosphorylate clusters on dPER that have distinct biochemical functions and effects on the rate of dPER degradation, e.g., elements such as the per-short phospho-cluster that delays dPER degradation and those such as the SLIMB-binding site and global phosphorylation that enhance instability. NMO plays a major role in the relative timing of DBT activity at these different elements because it stimulates multisite phosphorylation at the per-short delay cluster by DBT, which slows down the ability of DBT to phosphorylate instability elements. Thus, a large portion of the phosphorylation events dictating when in a daily cycle dPER is targeted for rapid degradation is not *directly* linked to binding of SLIMB per se. Our findings demonstrate that presumptive long-range interactions between distinct positively and negatively acting phospho-clusters collaborate to set clock speed and helps to explain why mutations in clock protein phosphorylation sites and/or the kinases that phosphorylate them can yield both fast and slow clocks.

Our proposed mechanism for the function of the per-short domain (Figure 6C) is supported by the congruence between *in vitro* biochemical studies based on purified recombinant dPER protein from cultured S2 cells and *in vivo* changes in the pace of behavioral rhythms using transgenic models. This suggests that a primary biochemical effect of the per-short domain on clock speed in the fly is via modulating the rate of DBT-mediated phosphorylation at the SLIMB phospho-degron on dPER. The physiological role of T583 phosphorylation is not clear, as mutating this site does not have detectable effects on the binding of dPER to SLIMB in S2 cells (Figure 1, Figure 2, and data not shown). In this regard, it is interesting to note that the original per-short domain was identified as encompassing aa 585–601 of dPER (Bayliss et al., 1992). Thus, it is likely that the 8 hr per-short delay circuit is governed by the dynamics underlying the phosphorylated status of three sites (i.e., S596, S589, and S585).

At present, it is not clear how phosphorylation in the per-short cluster slows down subsequent phosphorylation by DBT at Ser47 and other sites. Inactivating the per-short cluster leads to increases in the rate of DBT-mediated phosphorylation at not only the N terminus (Figure 2), but also the C terminus of dPER (data not shown), suggesting that it is a major control center for regulating the relative efficiency of DBT phosphorylation at many sites on dPER. We suggest that the per-short phospho-cluster acts as a transient “temporal trap” for DBT. Once the sites in the per-short domain are phosphorylated by DBT, this somehow allows it to continue its normal rate of phosphory-

lation at other phospho-clusters. Although speculative, progressive increases in phosphorylation at some of these other phospho-clusters might generate time-dependent local/overall conformational changes in dPER (Figure 7), possibly via electrostatic repulsion, eventually leading to a more open dPER structure that is more accessible to phosphorylation by DBT at the SLIMB-binding site and/or a more efficient substrate for degradation. Thus, the rapid degradation of dPER during the early day is likely due to a combination of synchronous increases in the phospho-occupancy of Ser47 and overall phosphorylation of dPER. Other factors such as protein phosphatases and the action of TIMELESS also play major roles in regulating the speed of the dPER phosphorylation program (Bae and Edery, 2006).

How might phosphorylation at S596 enhance phosphorylation at S589 and S585 by DBT? Phosphorylation by the CK1 kinase family is generally enhanced by priming (Flotow et al., 1990). However, phosphorylation at the per-short domain by DBT does not follow the consensus priming-dependent recognition motif for the CK1 family of kinases (i.e., S/Tp-X-X-S/T, wherein S/Tp refers to the primed site, X is any amino acid, and the italicized residues the CK1 target site [Flotow et al., 1990]), as the S596 priming site is located C terminal to the DBT sites. Thus, it is likely that phosphorylation of S596 by NMO stimulates DBT phosphorylation at the per-short region in a nonpriming-dependent manner. Ongoing studies are aimed at understanding the biochemical events underlying the ability of phosphorylation at S596 to enhance phosphorylation by DBT in the per-short region.

The discovery of a delay phospho-circuit also sheds light on why mutations in different phosphorylation sites on PER or FRQ proteins, although affecting stability, can speed up or slow down the clock (e.g., Baker et al., 2009; Chiu et al., 2008; Tang et al., 2009; Toh et al., 2001; Vanselow et al., 2006). Our findings also offer a logical explanation for why mutations that lower the kinase activity of CKI, which overall is expected to slow down the rate of PER degradation, can yield fast clocks. For example, although other mechanisms have been offered to explain the short-period phenotypes that are observed for the CKI ϵ^{tau} mutation in hamsters (Gallego et al., 2006; Meng et al., 2008) and a CKI δ mutation associated with familial advanced sleep phase syndrome (FASPS) in humans (Xu et al., 2005), it is possible that phosphorylation at a per-short type delay cluster is preferentially compromised by the mutant kinase, which could appear as a substrate-specific gain-of-function mutation.

Negatively acting phospho-clusters are likely to be a general feature of the timing mechanisms regulating the daily abundance cycles of clock proteins such as PERs in animals and FRQ in *Neurospora*. However, other regulatory modules that operate in a phase-specific manner must participate to generate an ~24 hr oscillator. Most conspicuously, clock speed is intimately linked to the PER and FRQ abundance cycles necessitating daily phases of *de novo* synthesis to replenish the pools of previously degraded proteins. As recently shown, the transcriptional negative feedback aspect of dPER regulating dCLK-CYC-mediated transcription is also a component of the period-setting mechanism (Kadener et al., 2008). Therefore, the ~24 hr dPER abundance cycle is based on a combination of “time constraints” that are generated using different regulatory modules. We propose that the per-short-based timer mainly functions once dPER has accumulated

and begins participating in transcriptional repression, controlling dPER abundance once it is disengaged from the dynamics of its cognate mRNA by setting in motion a series of sequential phosphorylation events that are calibrated to stimulate dPER degradation in the nucleus at the appropriate time in a daily cycle, enabling the next round of circadian gene expression. In this context, it is interesting to note that a prior study analyzing the per-short domain suggested that it functions with a nearby “perSD” domain to increase the transcriptional repressor function of dPER (Kivimäe et al., 2008). It is possible that the same phosphorylation events leading to dPER degradation also function to increase its potency within the repressor complex.

Our studies also identify NEMO as a clock kinase. NEMO is the founding member of the evolutionarily conserved Nemo-like kinase (Nlk) family of proline-directed serine/threonine kinases closely related to mitogen-activated protein kinases (MAPK) (Brott et al., 1998). It was originally characterized in *Drosophila* as required for planar cell polarity during eye development (Choi and Benzer, 1994) and is now known to function in many pathways. Nmo/Nlk is localized in the nucleus (Brott et al., 1998) and is another factor in the circadian clock that also functions in the Wnt/Wg-signaling pathway (Thorpe and Moon, 2004; Zeng and Verheyen, 2004), such as CKI ϵ /DBT, β -TrCP/SLIMB, and GSK-3 β /SGG. It will be of interest to determine whether Nlk functions in the mammalian clock. Intriguingly, the phosphorylation sites on dPER are largely clustered, and several of them have the same spatial arrangement as the per-short cluster, with a predicted pro-directed kinase site at the C-terminal end of the phospho-cluster (Chiu et al., 2008). This suggests that Nmo and/or other pro-directed kinases serve as control points to activate spatially and perhaps functionally distinct phospho-clusters (Figure 6 and data not shown). Indeed, we recently showed that phosphorylation at Ser661 of dPER by an as yet unidentified pro-directed kinase primes further phosphorylation by SGG at Ser657 to regulate the timing of dPER nuclear entry in key pacemaker neurons (Ko et al., 2010).

In summary, a central aspect of circadian clocks is the presence of one or more clock proteins that provide a dual function by behaving as phospho-based timers and linking its timer role to gene expression by operating in a phase-specific manner to recruit repressor complexes that inhibit central clock transcription factors. Our studies suggest that a major part of the timing mechanism underlying these phospho-clock proteins is based on spatially and functionally discrete phospho-clusters that interact to impose calibrated and sequentially ordered biochemical time constraints. In the case of dPER, the per-short phospho-cluster functions as a central timing module by slowing down the ability of DBT to phosphorylate instability elements regulating dPER degradation and, hence, when dPER repressor activity is terminated and the next round of circadian gene expression begins.

EXPERIMENTAL PROCEDURES

S2 Cell Culture and Transfection

S2 cells and DES expression medium were obtained from Invitrogen, and transient transfections were performed using Effectene (QIAGEN) according to manufacturer's instructions and as previously described (Chiu et al.,

2008; Ko et al., 2002). For each transient transfection, 0.8 μ g of different *dper*-containing plasmids and 0.2 μ g of pMT-*dbt*-V5-His or empty control pMT-V5-His plasmids were used. For expression of proline-directed kinases, 0.4 μ g of plasmids were used. Expression of *dbt* and other kinases under pMT promoter was induced by adding 500 μ M CuSO₄ to the culture media 36 hr after transfection. Stable cell lines expressing pMT-*gst-slimb* were generated using calcium phosphate transfection kit (Invitrogen), and induction of pMT-driven expression was achieved using 500 μ M CuSO₄. For experiments in which the proteasome inhibitor MG132 (50 μ M; Sigma) and cycloheximide (10 μ g/ml; Sigma) were used (Figure 2, Figure 4A, Figure S2A, Figure S4, and Figure S5A), they were added 4 hr prior to cell harvest.

Transgenic Flies and Locomotor Activity Assays

Transgenic flies carrying *dper* mutations were generated as described in greater detail in the Extended Experimental Procedures. Fly locomotor activity rhythms were measured using the *Drosophila* Activity Monitoring (DAM) System from Trikinetics (Chiu et al., 2010).

Generation of Phospho-Specific Antibodies and Immunoblotting

Phospho-specific antibodies were generated by Proteintech Group, Inc. (USA). Rabbits were immunized with three different peptides to generate three different phospho-specific antibodies: pS585 = N'-C-PHENELTVpSERDSVM, pS589 = N'-C-ELTVSERDpSVMLGEI, and pS596 = N'-C-VMLGEIpSPHHDDYDS (wherein p = phosphate). Immunoblotting analysis was performed as previously described (Lee et al., 1998) with modifications detailed in the Extended Experimental Procedures. The guinea pig α -dPER antibodies (GP339 and GP73) were previously described (Ko et al., 2010; Sidote et al., 1998).

Immunoprecipitation and Phosphatase Treatment

Immunoprecipitation and phosphatase treatment were performed as described (Lee et al., 1998) with modifications detailed in the Extended Experimental Procedures.

TEV Enzyme Cleavage and GST Pull-Down Assay

TEV cleavage and GST-SLIMB binding assays were performed as previously described (Chiu et al., 2008).

In Vitro Kinase Assay

S2 cells were transiently transfected with *pAc-dper-V5-His*. S2 cells were harvested 48 hr after transfection, and dPER proteins were extracted using EB2 (see the Extended Experimental Procedures). After IP with α -V5 agarose (Sigma) (see the Extended Experimental Procedures) to obtain dPER proteins, samples were subjected to λ -PP (NEB) or mock treatment at 30°C for 30 min. Samples were subsequently washed two times with appropriate reaction buffers (NLK from Millipore and CDC2, MAPK, and GSK3 β from NEB). Kinase assays were performed at 30°C for 30 min following the manufacturer's suggested protocol.

SUPPLEMENTAL INFORMATION

Supplemental Information includes Extended Experimental Procedures, six figures, and one table and can be found with this article online at doi:10.1016/j.cell.2011.04.002.

ACKNOWLEDGMENTS

We thank Paul Hardin (Texas A&M, USA) for communicating unpublished results (Yu et al., 2011), Thomas Kusch (Rutgers University, USA) for Sfx cells, and the VDRC (Vienna, Austria) for RNAi lines. We thank Axel Diernfellner and Michael Brunner (Heidelberg University, Germany) for conditions for limited proteolysis. This work was supported by NIH grant (R01NS03498) to I.E. and NIH grant (K99/R00NS061952) to J.C.C.

Received: December 24, 2010

Revised: March 27, 2011

Accepted: April 1, 2011

Published online: April 21, 2011

REFERENCES

- Allada, R., and Chung, B.Y. (2010). Circadian organization of behavior and physiology in *Drosophila*. *Annu. Rev. Physiol.* **72**, 605–624.
- Bae, K., and Edery, I. (2006). Regulating a circadian clock's period, phase and amplitude by phosphorylation: insights from *Drosophila*. *J. Biochem.* **140**, 609–617.
- Baker, C.L., Kettenbach, A.N., Loros, J.J., Gerber, S.A., and Dunlap, J.C. (2009). Quantitative proteomics reveals a dynamic interactome and phase-specific phosphorylation in the *Neurospora* circadian clock. *Mol. Cell* **34**, 354–363.
- Baylies, M.K., Bargiello, T.A., Jackson, F.R., and Young, M.W. (1987). Changes in abundance or structure of the *per* gene product can alter periodicity of the *Drosophila* clock. *Nature* **326**, 390–392.
- Baylies, M.K., Vosshall, L.B., Sehgal, A., and Young, M.W. (1992). New short period mutations of the *Drosophila* clock gene *per*. *Neuron* **9**, 575–581.
- Blau, J., and Young, M.W. (1999). Cycling vrille expression is required for a functional *Drosophila* clock. *Cell* **99**, 661–671.
- Brand, A.H., and Perrimon, N. (1993). Targeted gene expression as a means of altering cell fates and generating dominant phenotypes. *Development* **118**, 401–415.
- Brott, B.K., Pinsky, B.A., and Erikson, R.L. (1998). Nlk is a murine protein kinase related to Erk/MAP kinases and localized in the nucleus. *Proc. Natl. Acad. Sci. USA* **95**, 963–968.
- Brunner, M., and Schafmeier, T. (2006). Transcriptional and post-transcriptional regulation of the circadian clock of cyanobacteria and *Neurospora*. *Genes Dev.* **20**, 1061–1074.
- Chiu, J.C., Vanselow, J.T., Kramer, A., and Edery, I. (2008). The phosphorylation occupancy of an atypical SLIMB-binding site on PERIOD that is phosphorylated by DOUBLETIME controls the pace of the clock. *Genes Dev.* **22**, 1758–1772.
- Chiu, J.C., Low, K.H., Pike, D.H., Yildirim, E., and Edery, I. (2010). Assaying locomotor activity to study circadian rhythms and sleep parameters in *Drosophila*. *J. Vis. Exp.* Published online September 28, 2010. 10.3791/2157.
- Choi, K.W., and Benzer, S. (1994). Rotation of photoreceptor clusters in the developing *Drosophila* eye requires the *nemo* gene. *Cell* **78**, 125–136.
- Dietzl, G., Chen, D., Schnorrer, F., Su, K.C., Barinova, Y., Fellner, M., Gasser, B., Kinsey, K., Oettel, S., Scheiblaue, S., et al. (2007). A genome-wide transgenic RNAi library for conditional gene inactivation in *Drosophila*. *Nature* **448**, 151–156.
- Edery, I., Zwiebel, L.J., Dembinska, M.E., and Rosbash, M. (1994). Temporal phosphorylation of the *Drosophila* period protein. *Proc. Natl. Acad. Sci. USA* **91**, 2260–2264.
- Flotow, H., Graves, P.R., Wang, A.Q., Fiol, C.J., Roeske, R.W., and Roach, P.J. (1990). Phosphate groups as substrate determinants for casein kinase I action. *J. Biol. Chem.* **265**, 14264–14269.
- Gallego, M., and Virshup, D.M. (2007). Post-translational modifications regulate the ticking of the circadian clock. *Nat. Rev. Mol. Cell Biol.* **8**, 139–148.
- Gallego, M., Eide, E.J., Woolf, M.F., Virshup, D.M., and Forger, D.B. (2006). An opposite role for tau in circadian rhythms revealed by mathematical modeling. *Proc. Natl. Acad. Sci. USA* **103**, 10618–10623.
- Grima, B., Lamouroux, A., Chélot, E., Papin, C., Limbourg-Bouchon, B., and Rouyer, F. (2002). The F-box protein *slimb* controls the levels of clock proteins period and timeless. *Nature* **420**, 178–182.
- Hamblen, M.J., White, N.E., Emery, P.T., Kaiser, K., and Hall, J.C. (1998). Molecular and behavioral analysis of four period mutants in *Drosophila melanogaster* encompassing extreme short, novel long, and unorthodox arrhythmic types. *Genetics* **149**, 165–178.
- Heintzen, C., and Liu, Y. (2007). The *Neurospora crassa* circadian clock. *Adv. Genet.* **58**, 25–66.
- Kadener, S., Menet, J.S., Schoer, R., and Rosbash, M. (2008). Circadian transcription contributes to core period determination in *Drosophila*. *PLoS Biol.* **6**, e119.
- Kannan, N., and Neuwald, A.F. (2004). Evolutionary constraints associated with functional specificity of the CMGC protein kinases MAPK, CDK, GSK, SRPK, DYRK, and CK2alpha. *Protein Sci.* **13**, 2059–2077.
- Kim, E.Y., Ko, H.W., Yu, W., Hardin, P.E., and Edery, I. (2007). A DOUBLETIME kinase binding domain on the *Drosophila* PERIOD protein is essential for its hyperphosphorylation, transcriptional repression, and circadian clock function. *Mol. Cell Biol.* **27**, 5014–5028.
- Kivimäe, S., Saez, L., and Young, M.W. (2008). Activating PER repressor through a DBT-directed phosphorylation switch. *PLoS Biol.* **6**, e183.
- Kloss, B., Price, J.L., Saez, L., Blau, J., Rothenfluh, A., Wesley, C.S., and Young, M.W. (1998). The *Drosophila* clock gene double-time encodes a protein closely related to human casein kinase Iepsilon. *Cell* **94**, 97–107.
- Ko, H.W., and Edery, I. (2005). Analyzing the degradation of PERIOD protein by the ubiquitin-proteasome pathway in cultured *Drosophila* cells. *Methods Enzymol.* **393**, 394–408.
- Ko, H.W., Jiang, J., and Edery, I. (2002). Role for *slimb* in the degradation of *Drosophila* Period protein phosphorylated by Doubletime. *Nature* **420**, 673–678.
- Ko, H.W., DiMassa, S., Kim, E.Y., Bae, K., and Edery, I. (2007). Cis-combination of the classic *per(S)* and *per(L)* mutations results in arrhythmic *Drosophila* with ectopic accumulation of hyperphosphorylated PERIOD protein. *J. Biol. Rhythms* **22**, 488–501.
- Ko, H.W., Kim, E.Y., Chiu, J., Vanselow, J.T., Kramer, A., and Edery, I. (2010). A hierarchical phosphorylation cascade that regulates the timing of PERIOD nuclear entry reveals novel roles for proline-directed kinases and GSK-3beta/SGG in circadian clocks. *J. Neurosci.* **30**, 12664–12675.
- Konopka, R.J., and Benzer, S. (1971). Clock mutants of *Drosophila melanogaster*. *Proc. Natl. Acad. Sci. USA* **68**, 2112–2116.
- Konopka, R.J., Hamblen-Coyle, M.J., Jamison, C.F., and Hall, J.C. (1994). An ultrashort clock mutation at the period locus of *Drosophila melanogaster* that reveals some new features of the fly's circadian system. *J. Biol. Rhythms* **9**, 189–216.
- Lee, C., Bae, K., and Edery, I. (1998). The *Drosophila* CLOCK protein undergoes daily rhythms in abundance, phosphorylation, and interactions with the PER-TIM complex. *Neuron* **21**, 857–867.
- Markson, J.S., and O'Shea, E.K. (2009). The molecular clockwork of a protein-based circadian oscillator. *FEBS Lett.* **583**, 3938–3947.
- Marrus, S.B., Zeng, H., and Rosbash, M. (1996). Effect of constant light and circadian entrainment of *perS* flies: evidence for light-mediated delay of the negative feedback loop in *Drosophila*. *EMBO J.* **15**, 6877–6886.
- Mehra, A., Baker, C.L., Loros, J.J., and Dunlap, J.C. (2009). Post-translational modifications in circadian rhythms. *Trends Biochem. Sci.* **34**, 483–490.
- Meng, Q.J., Logunova, L., Maywood, E.S., Gallego, M., Lebiecki, J., Brown, T.M., Sládek, M., Semikhodskii, A.S., Glossop, N.R., Piggins, H.D., et al. (2008). Setting clock speed in mammals: the CK1 epsilon tau mutation in mice accelerates circadian pacemakers by selectively destabilizing PERIOD proteins. *Neuron* **58**, 78–88.
- Nawathean, P., Stoleru, D., and Rosbash, M. (2007). A small conserved domain of *Drosophila* PERIOD is important for circadian phosphorylation, nuclear localization, and transcriptional repressor activity. *Mol. Cell Biol.* **27**, 5002–5013.
- Price, J.L., Blau, J., Rothenfluh, A., Abodeely, M., Kloss, B., and Young, M.W. (1998). double-time is a novel *Drosophila* clock gene that regulates PERIOD protein accumulation. *Cell* **94**, 83–95.
- Rosato, E., and Kyriacou, C.P. (2006). Analysis of locomotor activity rhythms in *Drosophila*. *Nat. Protoc.* **1**, 559–568.
- Rothenfluh, A., Abodeely, M., and Young, M.W. (2000). Short-period mutations of *per* affect a double-time-dependent step in the *Drosophila* circadian clock. *Curr. Biol.* **10**, 1399–1402.

- Rutila, J.E., Edery, I., Hall, J.C., and Rosbash, M. (1992). The analysis of new short-period circadian rhythm mutants suggests features of *D. melanogaster* period gene function. *J. Neurogenet.* *8*, 101–113.
- Schibler, U. (2006). Circadian time keeping: the daily ups and downs of genes, cells, and organisms. *Prog. Brain Res.* *153*, 271–282.
- Sidote, D., Majercak, J., Parikh, V., and Edery, I. (1998). Differential effects of light and heat on the *Drosophila* circadian clock proteins PER and TIM. *Mol. Cell Biol.* *18*, 2004–2013.
- Tang, C.T., Li, S., Long, C., Cha, J., Huang, G., Li, L., Chen, S., and Liu, Y. (2009). Setting the pace of the *Neurospora* circadian clock by multiple independent FRQ phosphorylation events. *Proc. Natl. Acad. Sci. USA* *106*, 10722–10727.
- Thorpe, C.J., and Moon, R.T. (2004). nemo-like kinase is an essential co-activator of Wnt signaling during early zebrafish development. *Development* *131*, 2899–2909.
- Toh, K.L., Jones, C.R., He, Y., Eide, E.J., Hinz, W.A., Virshup, D.M., Ptáček, L.J., and Fu, Y.H. (2001). An hPer2 phosphorylation site mutation in familial advanced sleep phase syndrome. *Science* *291*, 1040–1043.
- Vanselow, K., Vanselow, J.T., Westermarck, P.O., Reischl, S., Maier, B., Korte, T., Herrmann, A., Herzog, H., Schlosser, A., and Kramer, A. (2006). Differential effects of PER2 phosphorylation: molecular basis for the human familial advanced sleep phase syndrome (FASPS). *Genes Dev.* *20*, 2660–2672.
- Xu, Y., Padiath, Q.S., Shapiro, R.E., Jones, C.R., Wu, S.C., Saigoh, N., Saigoh, K., Ptáček, L.J., and Fu, Y.H. (2005). Functional consequences of a CK1delta mutation causing familial advanced sleep phase syndrome. *Nature* *434*, 640–644.
- Xu, Y., Toh, K.L., Jones, C.R., Shin, J.Y., Fu, Y.H., and Ptáček, L.J. (2007). Modeling of a human circadian mutation yields insights into clock regulation by PER2. *Cell* *128*, 59–70.
- Yu, Q., Jacquier, A.C., Citri, Y., Hamblen, M., Hall, J.C., and Rosbash, M. (1987). Molecular mapping of point mutations in the period gene that stop or speed up biological clocks in *Drosophila melanogaster*. *Proc. Natl. Acad. Sci. USA* *84*, 784–788.
- Yu, W., Hou, J.H., and Hardin, P.E. (2011). NEMO kinase contributes to core period determination by slowing the pace of the *Drosophila* circadian oscillator. *Curr. Biol.* *21*, in press. 10.1016/j.cub.2011.02.037.
- Zeng, Y.A., and Verheyen, E.M. (2004). Nemo is an inducible antagonist of Wingless signaling during *Drosophila* wing development. *Development* *131*, 2911–2920.